Soft Matter

RSC Publishing

PAPER

View Article Online
View Journal | View Issue

Discretizing elastic chains for coarse-grained polymer models

Cite this: *Soft Matter*, 2013, **9**, 7016

Elena F. Koslover*[a] and Andrew J. Spakowitz*[ab]

Studying the statistical and dynamic behavior of semiflexible polymers under complex conditions generally requires discretizing the polymer into a sequence of beads for purposes of simulation. We present a novel approach for generating coarse-grained, discretized polymer models designed to reproduce the polymer statistics at intermediate to long lengths. Our versatile model allows for an arbitrary discretization length and is accurate over a larger range of length scales than the traditional bead–rod and bead–spring models. In its generality, the discrete, stretchable, shearable wormlike chain (dssWLC) model incorporates the anisotropic elasticity inherent in a semielastic chain on intermediate length scales. We demonstrate quantitatively the statistical accuracy of this model at different discretizations, thereby allowing for efficient selection of the number of segments to be simulated. The approach presented in this work provides a systematic procedure for generating coarse-grained discrete models to probe physical properties of a semielastic polymer at arbitrary length scales.

Received 30th January 2013
Accepted 9th April 2013

DOI: 10.1039/c3sm50311a

www.rsc.org/softmatter

I Introduction

Many of the polymers commonly encountered in the biological context and elsewhere exhibit semiflexible properties. That is, they are effectively rigid, with a linear bending elasticity on some short length scale, begin to look increasingly flexible at longer lengths, and can be approximated as fully flexible threads at the longest length scales. Such polymers are often modeled as "wormlike chains" (WLC),[1,2] continuous chains with an energy density that is quadratic in the curvature and characterized by the persistence length ℓ_p – the length scale at which the polymer transitions from rigid to flexible behavior. The WLC model has been shown to be an effective description of a variety of locally stiff polymers, including double-stranded DNA[3–5] and RNA,[6] actin filaments,[7] unstructured polypeptides,[8] and carbon nanotubes.[9]

The statistical mechanics of the pure WLC model have been studied extensively,[2,10,11] with the partition function analytically calculated under various end constraints.[12–14] However, the incorporation of more complicated effects for realistic polymers, such as sterics, hydrodynamics, confinement, or interactions with packaging proteins, generally requires numerical simulation of the chain properties. For purposes of simulation, the wormlike chain is generally represented by a linear sequence of beads connected by an effective potential. Such discrete chains constitute a coarse-grained model of the polymer in question, as each bead generally represents a segment of the original detailed polymer containing many atoms. Simulations based on the WLC model have been employed to study the packing of DNA into chromatin fibers,[15,16] the packaging of viral genomes,[17] and the mechanical properties of actin networks.[18,19]

Two common approaches are employed for generating discrete versions of the wormlike chain model. The "bead–rod" models connect beads along the polymer contour with stiff rods and incorporate a bending potential between subsequent rods.[20] A closely related set of models allows for elastic stretching of the connected segments, with the stretch modulus set equal to that of the polymer being modelled.[15,19] When applied to modeling biopolymers such as DNA or actin filaments, the stretch modulus is usually quite high, approximating the bead–rod model. This potential is often harmonic in the bend angle, and such models can accurately reproduce the continuous wormlike chain provided that the segment length is significantly shorter than the persistence length. However, such an approach becomes computationally prohibitive when the total chain length is much longer than the length-scale of the polymer stiffness. For instance, the bead–rod model is impractical for modeling genomic DNA which can range from 10^4 to 10^7 persistence lengths. Another class of models represents the chain as beads connected by isotropic harmonic springs.[3,20,21] These models are essentially equivalent to mapping the polymer onto an effective Gaussian chain,[22] and can accurately represent chain behavior only when each bead represents a contour length significantly larger than the persistence length. Finer discretization can be achieved by modified bead–spring models which make use of alternative, non-harmonic spring force laws extracted from the force–extension behavior of the wormlike chain.[23,24]

[a]*Biophysics Program, Stanford University, Stanford, CA 94305, USA. E-mail: lenafabr@stanford.edu; ajspakow@stanford.edu*

[b]*Chemical Engineering Department, Stanford University, Stanford, CA 94305, USA*

The appropriate choice of discretization length (Δ) for a polymer chain arises from a balance between the available computational power and the length-scales relevant to the physics of interest. Increasing values of Δ result in a chain with fewer degrees of freedom, leading to more efficient simulations. However the minimal length-scale of accuracy will also increase as the discretization length increases. Currently, there is no standard approach to generating discrete chain models in a way that can incorporate both fine-grained and coarse-grained discretization within a single unified framework.

The process of generating a discrete model to represent a continuous chain can be thought of as a coarse-graining procedure. One seeks a representation of the chain that is accurate at length scales above the discretization length while forgoing accuracy at shorter length scales. In a previous work, we presented a systematic procedure for coarse-graining polymer models by mapping onto a family of continuous chains termed the stretchable, shearable wormlike chain (ssWLC) model.[25] The ssWLC is defined by both a position and an orientation vector at each point along the contour, with the energy for a given path containing quadratic penalties for bending of the orientation, stretching of the position along the orientation vector, shearing away from the orientation vector, and quadratic coupling between bend and shear deviations. We showed that such a chain, which incorporates both the classic Kratky–Porod wormlike chain and the Gaussian chain as special limits, can be used reproduce the intermediate to long-length statistics of any polymer defined entirely by localized interactions. The ssWLC provided a systematic approach to describing the behavior of complicated polymer chains by mapping to an analytically tractable continuous model.

In this work we describe a novel polymer model – the discrete, stretchable, shearable wormlike chain (dssWLC) – which serves as a discrete analog to the continuous ssWLC. The new model can be used to systematically generate discrete representations of the continuous wormlike chain at any desired length-scale of discretization. We provide a quantitative estimate of the length scale of accuracy for this model and show that the dssWLC can span length scales where neither bead–rod nor Gaussian spring models are accurate. Our discretization procedure is based on selecting effective parameters for the model in such a way as to match the intermediate to long-length statistics of the original polymer model being studied. Although we focus here on the discretization of the continuous wormlike chain, the methodology described could be employed to develop coarse-grained discrete models for an arbitrary polymer with semielastic properties, provided the physics defining its local behavior are known.

II Discrete models for the WLC

One of the most common approaches for creating a discretized version of the continuous WLC polymer model involves simply discretizing the Hamiltonian. For a chain of length L and discretization length Δ, the polymer is split into beads numbered from 0 to $N = L/\Delta$, separated by segments of fixed length. The polymer configuration is given by the bead positions $\{\vec{r}_i\}$ or equivalently by the orientations of the segments connecting adjacent beads $\vec{u}_i = (\vec{r}_i - \vec{r}_{i-1})/\Delta$. The free energy associated with a particular configuration is given by,

$$E(\{\vec{u}_i\}) = \sum_{i=1}^{N} \frac{\varepsilon_b}{2\Delta}\left|\vec{u}_i - \vec{u}_{i-1}\right|^2, \tag{1}$$

where ε_b is commonly set to equal to persistence length (ℓ_p) of the original wormlike chain.

Although such a "bead–rod" model is accurate for very fine-grained discretizations, the long-chain statistics of this discrete model diverge from those of the continuous WLC as the segment length Δ increases. In particular, the lowest-order moment of the end-to-end distance for the bead–rod chain can be calculated as,

$$\begin{aligned} \langle R^2 \rangle &= N\Delta^2 \frac{1+\xi}{1-\xi} + 2\Delta^2 \xi \frac{\xi^N - 1}{(1-\xi)^2}, \\ \xi &= \langle \vec{u}_i \cdot \vec{u}_{i-1} \rangle = \coth\left(\frac{\varepsilon_b}{\Delta}\right) - \frac{\Delta}{\varepsilon_b}. \end{aligned} \tag{2}$$

The long-chain statistics of the polymer are encompassed in the term of this lowest order moment that is linear in the chain length (here denoted as $C_2^{(1)}$). This term is also known as the effective Kuhn length,[22] and finding $C_2^{(1)}$ for a particular model is equivalent to mapping onto an effective Gaussian chain. In Fig. 1a we demonstrate how this term diverges from the value associated with a continuous wormlike chain as Δ increases. To properly reproduce the long-chain behavior, one must adjust the bending modulus ε_b in order to match the effective Kuhn length of the continuous chain,

$$C_2^{(1)} = \Delta\left(\frac{1+\xi}{1-\xi}\right) = 2\ell_p. \tag{3}$$

The appropriate bending modulus obtained by solving eqn (3) is plotted in Fig. 1a. We note that this bending modulus departs substantially from the continuous persistence length near $\Delta = 0.5\ell_p$, and decreases to zero as $\Delta \to 2\ell_p$. Equivalently, the WLC has the same effective Gaussian behavior at long length as the freely jointed chain with segment length $2\ell_p$. For segment lengths longer than $2\ell_p$, the bead–rod model cannot accurately reproduce long length-scale behaviour of the continuous WLC. The significance of adjusting the bending modulus as a function of the discretization length is shown in Fig. 1b, which compares the end-to-end distributions from discretized bead–rod chains using Monte Carlo simulations. The discrete model with the adjusted value of the bending modulus is notably more accurate at reproducing the statistics of the continuous WLC at low to intermediate chain extensions (corresponding to the longest length-scale effects).

We note that the adjustment of ε_b to reproduce the effective Kuhn length has been previously described.[26,27] We reiterate this analysis here because a large number of studies in recent literature continue to use the approximation $\varepsilon_b = \ell_p$ regardless of the discretization length. Furthermore the selection of the bending modulus to match long-length behavior provides a simple analogue for the more detailed discretization method that is the focus of the current work. All subsequent results in

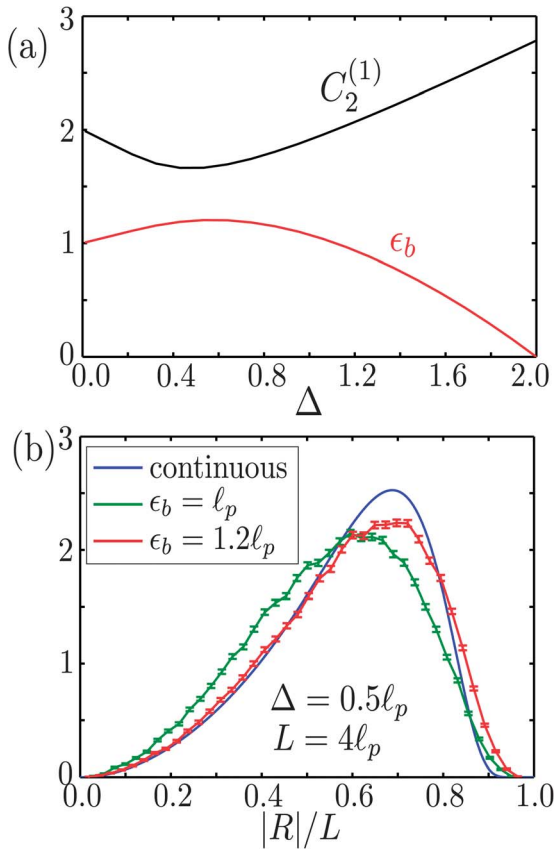

Fig. 1 Statistics of the bead–rod model. (a) Black: the linear term ($C_2^{(1)}$) of the mean square end to end distance, for different discretization lengths using the convention $\varepsilon_b = \ell_p$. Red: the appropriate value of ε_b to match the effective Kuhn length to that of the continuous WLC. All units are in terms of ℓ_p. (b) Distribution of the end-to-end distance for the bead–rod model with conventional (green) *versus* adjusted (red) values of the bending modulus, compared to the continuous WLC (blue), from Monte Carlo simulations of a chain of length $4\ell_p$ with segment length $\Delta = 0.5\ell_p$.

this work pertaining to the bead–rod model use the adjusted bending modulus obtained by solving eqn (3).

In order to more accurately reproduce the WLC statistics at intermediate length scales, it is necessary to match both the linear ($C_2^{(1)}$) and constant ($C_2^{(0)}$) terms of $\langle R_z^2 \rangle$, as well as the linear term ($C_4^{(1)}$) of the next highest order moment, $\langle R_z^4 \rangle$. If these three terms match between two chain models, then all moments of the end-to-end distance will match out to an error that scales as $\mathcal{O}(1/L^2)$ as a fraction of the long-length limit.[25] In order to develop a discrete chain model that can match these three constants, we require two additional free parameters in the model.

A natural choice is to consider a stretchable discrete WLC, where the segments between beads are allowed to stretch away from their preferred length, with a quadratic penalty. Such a model could reproduce more accurately the physics of the continuous WLC by incorporating the tendency of a chain segment of contour length Δ to be compressed, on average, as a result of thermal wiggles. Again, the chain configuration is given by a set of beads at positions $\{\vec{r}_i\}$, $i = 0,\ldots,N$. We define the free energy function for the discrete stretchable WLC as follows,

$$E\left(\left\{\vec{R}_i\right\}\right) = \sum_{i=1}^{N} \frac{\varepsilon_b}{2\Delta}\left|\vec{u}_i - \vec{u}_{i-1}\right|^2 + \frac{\varepsilon_\parallel}{2\Delta}\left(\left|\vec{R}_i\right| - \Delta\gamma\right)^2, \quad (4)$$

where $\vec{R}_i = \vec{r}_i - \vec{r}_{i-1}$ and $\vec{u}_i = \vec{R}_i/|\vec{R}_i|$. This model includes three parameters—the bending modulus (ε_b), the stretch modulus $\varepsilon_\parallel$, and the ground-state segment compression (γ). The low-order moments of the end-to-end distance for such a model can be calculated as described in Appendix A.

The effective parameters of the discrete stretchable WLC are obtained by matching the terms $C_2^{(1)} = 2/3\ell_p$, $C_2^{(0)} = -2/3{\ell_p}^2$, $C_4^{(1)} = -208/45{\ell_p}^3$ of the continuous WLC (see Fig. 2a). We see the ground state length γ of the segments decreases with increasing Δ as longer contour lengths are on average more compressed under thermal fluctuations. Interestingly, the bending modulus ε_b increases with Δ, though we note that the overall bending stiffness between adjacent segments (ε_b/Δ) does decrease for longer segments, as expected. This relative stiffening is a manifestation of the additional correlations beyond the Gaussian chain model (which has $C_2^{(0)} = C_4^{(1)} = 0$) that are imposed by matching these additional terms to those of the continuous WLC. As the segment length increases, the segments also become more flexible, with decreasing stretch

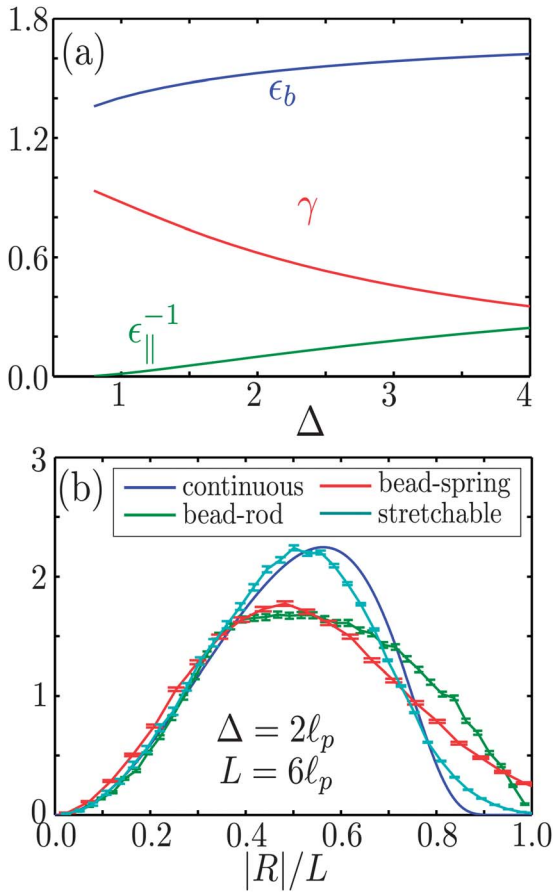

Fig. 2 Statistics for the discrete stretchable WLC model. (a) Effective parameters for discretizing a continuous WLC with discretization length Δ. All length units are in terms of ℓ_p. (b) Distribution of the end-to-end distance for a wormlike chain of length $6\ell_p$ with a discretization length of $\Delta = 2\ell_p$. The bead–rod model (green), bead–spring Gaussian model (red), and discrete stretchable WLC model (cyan) are compared to the analytic results for the continuous chain (blue).

modulus $\varepsilon_{\parallel}$. The improvement of the stretchable WLC over the standard bead–rod model or the isotropic bead–spring model obtained by mapping to a Gaussian chain is illustrated by the distribution of chain extensions obtained from Monte Carlo simulations (Fig. 2b).

We note that with this discretization procedure the stretch modulus becomes infinite as the segment length decreases down to $\Delta = 0.79\ell_p$. At this particular discretization length, the inextensible bead–rod model accurately reproduces the moments of the continuous chain out to the second highest order in chain length. The discrete stretchable WLC cannot be used to model the continuous WLC for segment lengths below this critical value, and a more complicated polymer model with additional parameters is required. In the subsequent section, we develop a discrete stretchable, shearable wormlike chain (dssWLC) model, which serves as a discretized version of the universal continuous elastic model used for coarse-graining of polymer chains in a previous work.[25] We show that this model allows us to reproduce the intermediate to long length behavior of the continuous WLC at arbitrary discretization length Δ.

III Discrete SSWLC model

The dssWLC model chain consists of a sequence of beads numbered 0 through N, with the polymer configuration fully described by the positions ($\vec{r}_i$) of each bead and the unit vectors ($\vec{u}_i$) attached to each bead. For convenience, we define the vectors connecting adjacent beads as $\vec{R}_i = \vec{r}_i - \vec{r}_{i-1}$. We note that the orientation vectors $\vec{u}_i$ constitute additional degrees of freedom in this model, and are not equal to the tangent vectors connecting the beads. The free energy function for a particular configuration of the polymer chain is given by,

$$E\left(\left\{\vec{R}_i, \vec{u}_i\right\}\right) = \sum_{i=1}^{N}\left[\frac{\varepsilon_b}{2\Delta}\left|\vec{u}_i - \vec{u}_{i-1} - \eta\vec{R}_i^{\perp}\right|^2 + \frac{\varepsilon_{\parallel}}{2\Delta}\left(\vec{R}_i\cdot\vec{u}_{i-1} - \Delta\gamma\right)^2 + \frac{\varepsilon_{\perp}}{2\Delta}\left|\vec{R}_i^{\perp}\right|^2\right] \quad (5)$$

where $\vec{R}_i^{\perp} = \vec{R}_i - (\vec{R}_i\cdot\vec{u}_{i-1})\,\vec{u}_{i-1}$ is the component of the interbead vector perpendicular to the orientation vector $\vec{u}_{i-1}$. This model, illustrated in Fig. 3, discretizes the continuous-chain Hamiltonian of the previously described ssWLC model.[25] Its six parameters include the bending modulus (ε_b), stretch modulus ($\varepsilon_{\parallel}$), shear modulus ($\varepsilon_{\perp}$), bend–shear coupling (η), and fractional ground-state segment length (γ), which serve analogous roles to the parameters in the continuous model. An additional parameter (Δ) corresponds to the discretization length—the continuous contour length encompassed by each segment of the discrete model. We note that when $\varepsilon_b = \ell_p$, $\gamma = 1$, $\varepsilon_{\parallel}$, $\varepsilon_{\perp} \to \infty$, the dssWLC reduces to the standard bead–rod model used to discretize a wormlike chain with persistence length ℓ_p.

The propagator for a single segment of the discrete chain can be defined as,

$$G_1(\vec{u}, \vec{R}|\vec{u}_0) = \frac{1}{\mathcal{N}}\exp\left[-E_1(\vec{u}, \vec{R}, \vec{u}_0)\right] \quad (6)$$

where $\mathcal{N}$ is a normalization constant and E_1 corresponds to the free energy for a single segment (the summand in eqn (5)). The partition function for the entire chain of N segments can then be found by a convolution of N copies of G_1,

$$G_N(\vec{u}, \vec{R}|\vec{u}_0) = \int \mathrm{d}\{\vec{r}_i\}\mathrm{d}\{\vec{u}_i\}\prod_{i=1}^{N} G_1(\vec{u}_i, \vec{r}_i - \vec{r}_{i-1}|\vec{u}_{i-1}) \quad (7)$$

To simplify the convolution structure we perform a Fourier transform $\vec{R} \to \vec{k}$. For simplicity, we assume that the wavevector is oriented along the $\hat{z}$ canonical axis ($\vec{k} = k\hat{z}$). The transformed single-segment propagator is given by,

$$\hat{G}_1(\vec{u}, k|\vec{u}_0) = \frac{1}{\mathcal{N}}\exp\left[\frac{\ell_p}{\Delta}\vec{u}\cdot\vec{u}_0 + \frac{\varepsilon_b^2\eta^2}{2\Delta\hat{\varepsilon}_{\perp}}\left[1 - (\vec{u}\cdot\vec{u}_0)^2\right] + ik\left\{\Delta\gamma\hat{z}\cdot\vec{u}_0 + \frac{\eta\varepsilon_b}{\hat{\varepsilon}_{\perp}}\left[\vec{u}\cdot\hat{z} - (\vec{u}\cdot\vec{u}_0)(\hat{z}\cdot\vec{u}_0)\right]\right\} - k^2\left\{\frac{\Delta}{2}\left(\frac{1}{\varepsilon_{\parallel}} - \frac{1}{\hat{\varepsilon}_{\perp}}\right)(\hat{z}\cdot\vec{u}_0)^2 + \frac{\Delta}{2\hat{\varepsilon}_{\perp}}\right\}\right] \quad (8)$$

where $\hat{\varepsilon}_{\perp} = \varepsilon_{\perp} + \eta^2\varepsilon_b$.

Furthermore, if we expand the propagator in terms of the spherical harmonics,[28]

$$\hat{G}_1(\vec{u}, k|\vec{u}_0) = \sum_{\ell_0,\ell,j} g^j_{\ell,\ell_0}\, Y^j_{\ell}(\vec{u})\, Y^{j*}_{\ell_0}(\vec{u}_0) \quad (9)$$

then the convolution in eqn (7) turns into a matrix multiplication and the overall partition function for the chain can be expressed as

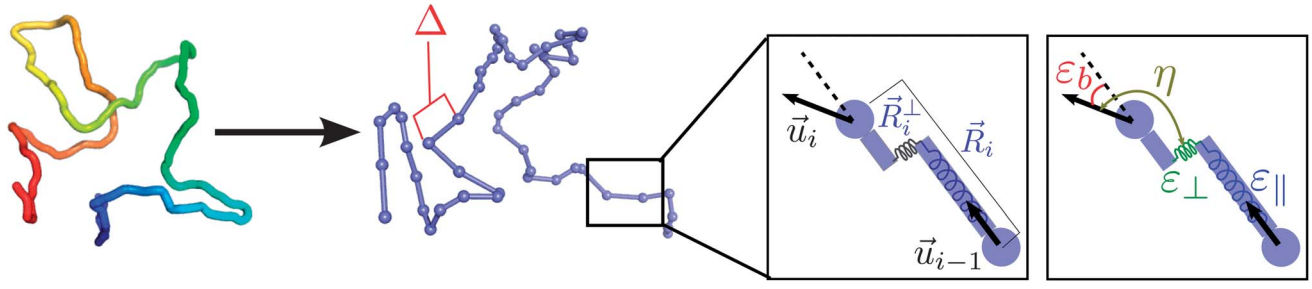

Fig. 3 Schematic of the discrete stretchable, shearable WLC model. The chain contour is discretized into beads separated by segments of length Δ, with each bead characterized by a position and an attached orientation vector $\vec{u}_i$. The free energy function incorporates quadratic penalties for stretch, shear, and bending deviations, as well as coupling between the bend and shear degrees of freedom.

$$\hat{G}_N(\vec{u},k|\vec{u}_0) = \sum \left[\left(\boldsymbol{g}^{(j)}\right)^N\right]_{\ell,\ell_0} Y_\ell^j(\vec{u})\, Y_{\ell_0}^{j*}(\vec{u}_0) \tag{10}$$

where $\boldsymbol{g}^{(j)}$ is the matrix of coefficients for the Fourier, spherical-harmonic transformed propagator. Note that throughout this manuscript we use boldfaced symbols for matrices. If we are interested specifically in the distribution of the N^{th} bead position (given by $\left[(\boldsymbol{g}^{(0)})^N\right]_{0,0}$), then we may assume $j = 0$, and this index is dropped for all subsequent calculations. This formulation is analogous to previously developed approaches for calculating the partition function of a chain consisting of linked segments by convolution over the degrees of freedom for the joints.[25,29] The defining physics of the specific discrete chain model used here is encompassed by the matrix $\boldsymbol{g}(k)$. Details on the calculation of the $g_{\ell,\ell_0}(k)$ coefficients for the dssWLC are provided in Appendix B.

Moments of the end-to-end displacement for the discrete chain are found, as in the continuous case, by taking derivatives of the coefficient $\boldsymbol{g}_{00}^N$ with respect to the wave-vector magnitude k (see Appendix C). The discrete chain structure factor is defined as the Fourier-transformed density correlation function,

$$\begin{aligned} S_{\text{dssWLC}}(k) &= \frac{2}{N^2}\sum_{n_1=0}^{N}\sum_{n_2=0}^{n_1}\left\langle \exp\left[ik\left(\vec{r}_{n_2}-\vec{r}_{n_1}\right)\cdot\hat{z}\right]\right\rangle \\ &= \frac{2}{N^2}\sum_{n_1=0}^{N}\sum_{n_2=0}^{n_1}\left[\boldsymbol{g}^{(n_2-n_1)}\right]_{0,0} \\ &= \left[\left\{N\boldsymbol{I}+\boldsymbol{g}^{(N+1)}-(N+1)\boldsymbol{g}\right\}\cdot(\boldsymbol{g}-\boldsymbol{I})^{-2}\right]_{0,0} \end{aligned} \tag{11}$$

where $\boldsymbol{I}$ is the identity matrix.

IV Discretizing with the DSSWLC model

In a previous work,[25] we described how to coarse-grain a polymer chain by mapping to the continuous ssWLC model, using the effective persistence length ℓ_p as a sliding parameter to set the degree of coarse-graining. Here, we proceed in an analogous fashion, by finding the effective parameters ε_b, $\varepsilon_\parallel$, $\varepsilon_\perp$, η, γ of the dssWLC in such a way as to ensure that all moments of the end-to-end distribution match up to the second highest order in chain length. For simplicity, we non-dimensionalize length units such that the continuous chain has a persistence length of 1. We note that the effective persistence length (ℓ_p^{eff}) of the discrete chain can be defined as

$$\left\langle \vec{u}_i\cdot\vec{u}_{i-1}\right\rangle = g_{11}(k=0) = \exp\left(-\frac{\Delta}{\ell_p^{\text{eff}}}\right). \tag{12}$$

Continuing the analogy to the continuous ssWLC, we define a dimensionless parameter $\alpha = \eta^2\varepsilon_b/\varepsilon_\perp$, so that the effective persistence length depends only on ε_b, α. For fixed values of ℓ_p^{eff}, α, the components of the low-order moments can be expressed as polynomial functions (of order 8 or lower) in the remaining three parameters, γ, ${\varepsilon_\parallel}^{-1}$, ${\varepsilon_\perp}^{-1}$ (see Appendix D). We solve these coupled polynomial equations to find the effective parameters of the dssWLC model that will reproduce the continuous chain at intermediate to long lengths. Since ℓ_p^{eff} served as an indication of the coarse-graining scale for the continuous chain mapping, we proceed to select the lowest possible value of ℓ_p^{eff} such that a solution exists with $\gamma > 0$, $\varepsilon_\parallel > 0$, $\varepsilon_\perp > 0$.

In order to quantify the length-scale of accuracy for the dssWLC model, we examine the structure factor as compared to that of the continuous WLC. The discretized structure factor for the continuous WLC ($S_{\text{cont}}(k)$) is defined as in eqn (11), with the Fourier, spherical-harmonic transformed propagator $\boldsymbol{g}$ taken to be the previously characterized[11] propagator for a continuous chain of length Δ. Fig. 4 shows the fractional error in the structure factor,

$$E_{\text{model}}(k) = \frac{S_{\text{model}}(k) - S_{\text{cont}}(k)}{S_{\text{cont}}(k)}, \tag{13}$$

as a function of the wavevector magnitude k, for both the dssWLC and the bead–rod models. Small values of k correspond to long length-scale behavior, while larger values dial in statistics for progressively shorter length-scales. The dssWLC outperforms the bead–rod model, with the difference between the two increasing significantly as the discretization length Δ is increased. We define the length-scale of accuracy for each model as $\lambda_{\text{model}} = 1/k^*$ where $E_{\text{model}} < 10^{-4}$ for all $k < k^*$. That is, we pick a cutoff for accuracy in the structure factor and find the length-scale such that the model exceeds that accuracy at all longer lengths.

Up to this point, in selecting the effective parameters of the dssWLC model, we have set the parameter α to an arbitrary fixed constant. Using the above definition of the length-scale of accuracy, we can now allow α to vary for each discretization length in such a way as to minimize λ_{dssWLC}. The resulting effective parameters of the discrete model are plotted in Fig. 5. We note that for $\Delta \geq 1.8$, the shear modulus becomes infinite and the appropriate dssWLC model reduces to one where the orientation vectors $\vec{u}_i$ fully align with the bead-to-bead vectors. In this limit, the dssWLC model constitutes a modified version of the discrete stretchable WLC described in Section II. In Appendix E we describe a procedure for efficiently representing

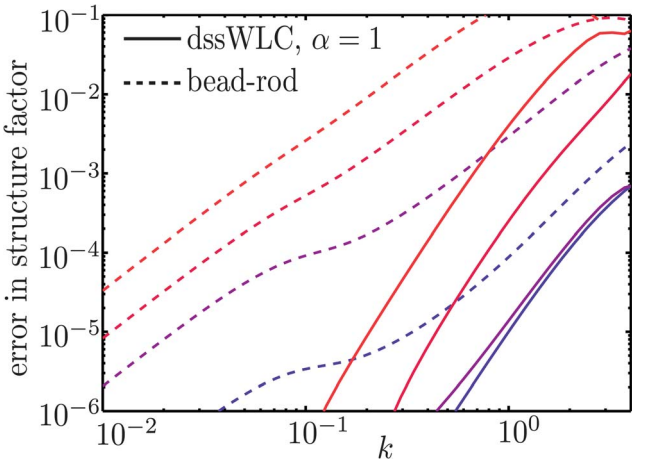

Fig. 4 Error in the structure factor (eqn (13)) for the bead–rod (dashed) and dssWLC models (solid), compared to the continuous WLC. Discretization lengths are $\Delta = 0.1, 0.5, 1, 2$ (from blue to red). A constant value of $\alpha = 1$ is used in these calculations.

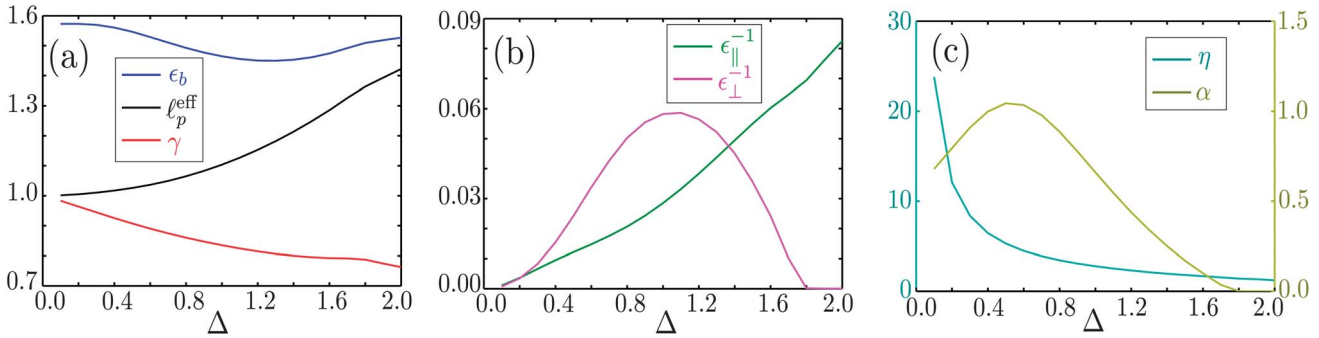

Fig. 5 Parameters for the dssWLC model for discretizing a continuous WLC at different discretization lengths Δ. The dimensionless parameter α is adjusted in such a way as to minimize the length scale of accuracy. (a) Bending modulus (blue), effective persistence length for the discrete chain (black), and ground state segment compression (red). (b) Inverse stretch (green) and shear (magenta) modulus. $\varepsilon_\perp{}^{-1} = 0$ corresponds to a modified discrete stretchable WLC model as described in Appendix E. (c) Coupling coefficient (cyan) and α parameter (yellow).

the dssWLC with $\varepsilon_\perp \to \infty$ in simulations without keeping track of the $\vec{u}$ orientation vectors.

For small values of the discretization length $\Delta \to 0$, the stretch and shear moduli become infinite, with the ground state compression $\gamma \to 1$, as expected for increasingly short segments of a semiflexible chain. The effective persistence length also approaches the original value for the continuous WLC $\ell_{\rm p}^{\rm eff} \to 1$ as the auxiliary vectors $\vec{u}_i$ attached to each bead become identical with the discrete tangent vectors connecting consecutive beads.

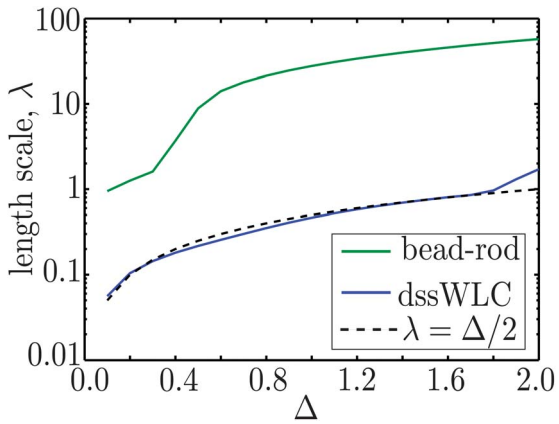

Fig. 6 Length scale of accuracy ($\lambda = 1/k^*$) for the bead–rod and the dssWLC model (with parameters given in Fig. 5) as a function of the discretization length. The line $\lambda = \Delta/2$ is also shown for comparison.

Finally, in Fig. 6 we plot the effective length-scale of accuracy for the dssWLC model with optimized values of α, as compared to the bead–rod model. We see that the minimal length-scale of accuracy for the bead–rod model rises sharply with increasing discretization length Δ, so that models with longer segments can only be efficiently applied for very long chains. The dssWLC model on the other hand, allows for discretization at any segment length Δ while remaining accurate at significantly shorter length-scales. The length-scale of accuracy for our model can be approximated as $\lambda \sim \Delta/2$ over the range $\Delta < 1.8$. The transition to a higher scaling with Δ occurs at the point where the shear modulus becomes infinite and the coarse-grained model becomes a modified version of the discrete stretchable chain (see Appendix E).

We further illustrate the utility of this model by comparing the distribution of end-to-end extensions for chains of intermediate length (Fig. 7). Although both models can reproduce this distribution at a fine-grained discretization of $\Delta = 0.1$, the dssWLC model allows the discretization length to increase by a

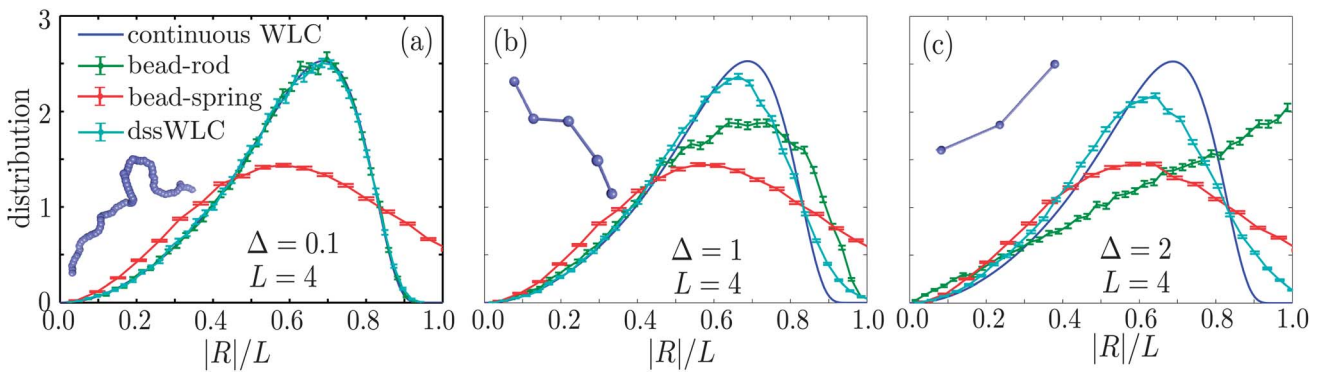

Fig. 7 Distributions of the end-to-end displacement for a chain of intermediate length ($L = 4$, in terms of the continuous chain persistence length). Analytic results for the continuous WLC are shown in blue. Monte Carlo simulations for the bead–rod model (green) and bead–spring model (red) and dssWLC model (cyan) are shown, using different discretization lengths.

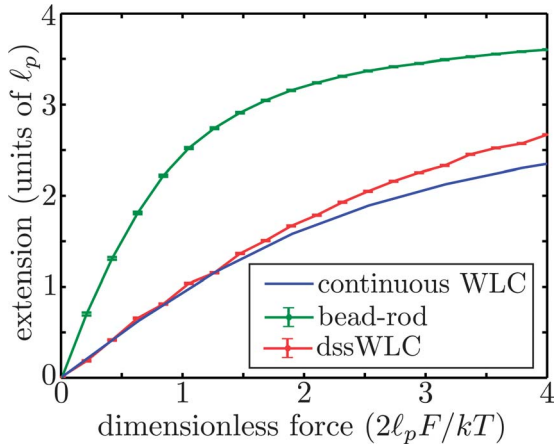

Fig. 8 Average extension along direction of applied force, for the continuous wormlike chain and simulated discrete models, using a discretization length $\Delta = 2\ell_p$ and total chain contour length $L = 4\ell_p$. Error bars are standard error of the mean from Monte Carlo simulations.

factor of 10–20 while still remaining relatively accurate. We note that the dssWLC model deviates from the continuous chain behavior at larger values of the end-to-end extension because this model does not include any finite length constraint preventing the segments from stretching beyond their contour length. The statistics of the chain near full extension are dominated by short length-scale wiggles, explaining the loss of accuracy in this regime.

As a further application of the discretization procedure described here, we consider the simulated force–extension curves for the dssWLC chain, the bead–rod chain, and the continuous wormlike chain (Fig. 8). Such curves are commonly used for interpreting single-molecule experiments that aim to extract mechanical properties of polymers such as DNA, RNA, or proteins by pulling on them *via* optical or magnetic traps.[3,5,6,30,31] Simulations of polymers under force have been employed for modeling the unpeeling of nucleosomes,[15] stretching and unfolding of chromatin,[32,33] and passage of DNA and other polymers through nanopores.[34] Our results show that the dssWLC model can accurately reproduce the low-force extension of the polymer at relatively large discretization lengths ($\Delta = 2$). Again, high force behavior is dominated by short length-scale fluctuations, so that coarse-grained models are inappropriate for studying this regime. In the low-force regime we see significantly improved agreement with the continuous chain statistics as compared to the bead–rod model.

V Concluding remarks

The results described in this manuscript demonstrate how the dssWLC model can be used to discretize a continuous semiflexible chain to an arbitrary segment length, with significantly improved accuracy in the chain statistics when compared to the conventional bead–rod model. We note that for a given discretization length, the dssWLC has two extra degrees of freedom per bead defining the additional orientation vector $\vec{u}_i$. However, while the total number of degrees of freedom in the simulation is less than doubled, the length scale of accuracy, as defined by comparison of the structure factor deviation from the continuous WLC, decreases by as much as 50-fold for segment lengths between one and two persistence lengths. Thus, the modest increase in complexity of the model is balanced by significant gains in accuracy. Overall, the dssWLC model allows for accurate simulation of the long-length behavior of the wormlike chain model at a significantly higher degree of coarse-graining and thus with a significant savings in computational time as compared to the standard approach of discretizing the chain into rigid segments.

The discretization method presented here has a wide range of possible applications in the field of polymer simulations. The appropriate discretization length Δ for any given application will depend on the length-scale of the relevant physics of interest. For instance, when simulating polymer networks or meshes, the discretization length needs to be smaller than the contour length separating interaction points or cross-links. One of the main strengths of the model described here is its universality, in that it can be applied to find an effective model at any given discretization length. By incorporating both fine-grained and coarse-grained discretizations within a single formalism, the dssWLC model opens up the possibility of adjusting the discretization between simulation runs with different parameter sets or even within an individual simulation as the relevant length-scale varies between different portions of the chain or different simulation time points.

A number of unanswered questions remain regarding efficient ways to incorporate non-local chain effects into simulations that make use of the dssWLC model with coarse discretization. For instance, the appropriate formulation of steric interactions for chains where each segment represents a relatively long contour length of the polymer of interest remains a topic for future study. We note that the same difficulties regarding steric interactions, topological constraints, and hydrodynamics plague the conventional discrete elastic models. One possibility that arises with the dssWLC is that of using finer discretization lengths in areas where the polymer chain becomes crowded or self-intersecting, while longer discretizations can be maintained in isolated regions of the polymer, with the discretization level adjusted dynamically throughout the simulation. Another approach would be to make use of the WLC propagator function to determine the shape of the chain density between fixed beads of the discrete model, using the result to create effective steric shapes for the segments connecting the beads. The dynamic behavior of the dssWLC is also an enticing topic for future study. A dynamic simulation making use of this model would require an effective friction coefficient for rotation of the orientation vectors $\vec{u}_i$.

The dssWLC model as presented here could, in principle, be expanded to include the twist of the polymer as well as its contour path. To this end the vectors $\vec{u}$ would need to be expanded to orthogonal triads representing a full coordinate orientation in space. The bending and shear moduli could then be made anisotropic with respect to this coordinate orientation. In addition to matching the moments of the end-to-end distance at long lengths, the additional parameters should make it possible to match moments of the coordinate orientation, so that the statistics of the polymer twist would also be reproduced at long length-scales. While such an expansion of

the model is beyond the scope of this manuscript, the use of the dssWLC to model polymers with twist, including global twist-writhe constraints remains a ripe topic for further study.

In a previous work we demonstrated how detailed polymer chains can be coarse-grained by mapping onto a continuous elastic polymer model with analytically tractable statistics.[25] Here we have presented an alternate, though closely related, approach that allows for mapping a continuous polymer model onto a discrete elastic chain suitable for simulations. The dssWLC allows the discretization, and thus the computational cost, of the simulation to be systematically adjusted to the minimal requirements necessary given the length-scale of interest. The discrete polymer model described here thus significantly expands our ability to model semiflexible polymer chains with the use of coarse-grained simulations.

$$\langle s\rangle = \frac{4 + 2\varepsilon_\parallel\gamma^2\Delta + \gamma\sqrt{\varepsilon_\parallel\Delta}\left(3 + \gamma^2\varepsilon_\parallel\Delta\right)X}{2\varepsilon_\parallel\gamma + \sqrt{\varepsilon_\parallel/\Delta}\left(1 + \gamma^2\varepsilon_\parallel\Delta\right)X} \tag{S4}$$

$$\langle s^2\rangle = \frac{10\gamma\Delta + 2\Delta^2\varepsilon_\parallel\gamma^3 + \sqrt{\Delta/\varepsilon_\parallel}\left(3 + 6\Delta\varepsilon_\parallel\gamma^2 + \Delta^2\varepsilon_\parallel^2\gamma^4\right)X}{2\varepsilon_\parallel\gamma + \sqrt{\varepsilon_\parallel/\Delta}\left(1 + \gamma^2\varepsilon_\parallel\Delta\right)X} \tag{S5}$$

$$\langle s^3\rangle = \frac{16\frac{\Delta}{\varepsilon_\parallel} + 18\Delta^2\gamma^2 + 2\Delta^3\varepsilon_\parallel\gamma^4 + \gamma\sqrt{\frac{\Delta^3}{\varepsilon_\parallel}}\left(15 + 10\Delta\varepsilon_\parallel\gamma^2 + \Delta^2\varepsilon_\parallel^2\gamma^4\right)X}{2\varepsilon_\parallel\gamma + \sqrt{\varepsilon_\parallel/\Delta}\left(1 + \gamma^2\varepsilon_\parallel\Delta\right)X} \tag{S6}$$

$$\langle s^4\rangle = \frac{66\frac{\gamma\Delta^2}{\varepsilon_\parallel} + 28\Delta^3\gamma^4 + 2\Delta^4\varepsilon_\parallel\gamma^5 + \sqrt{\frac{\Delta^3}{\varepsilon_\parallel^3}}\left(15 + 45\Delta\varepsilon_\parallel\gamma^2 + 15\Delta^2\varepsilon_\parallel\gamma^4 + \Delta^3\varepsilon_\parallel^3\gamma^6\right)X}{2\varepsilon_\parallel\gamma + \sqrt{\varepsilon_\parallel/\Delta}\left(1 + \gamma^2\varepsilon_\parallel\Delta\right)X} \tag{S7}$$

VI Appendix

A Low order moments of the discrete stretchable WLC

In this section we calculate the lowest-order moments $\langle {R_z}^2\rangle$ and $\langle {R_z}^4\rangle$ of the discrete stretchable WLC model, whose free energy function is defined by eqn (4). For convenience, we introduce the notation $s_i = |\vec{R}_i|$ for the length of segment i and $\rho_i = (\vec{R}_i\cdot\hat{z})/|\vec{R}_i|$ for the component of the segment orientation in the canonical $\hat{z}$ direction. Because the energy function has no coupling between the segment lengths and their orientations, the values of s_i and ρ_i are uncorrelated with each other. The low-order moments can then be expressed as

$$\langle {R_z}^2\rangle = \left\langle\left(\sum_{i=1}^{N} s_i\rho_i\right)^2\right\rangle = 2\langle s\rangle^2\sum_{i>j}\langle\rho_i\rho_j\rangle + N\langle s^2\rangle\langle {\rho_i}^2\rangle \tag{S1}$$

$$\begin{aligned}\langle {R_z}^4\rangle = \left\langle\left(\sum_{i=1}^{N} s_i\rho_i\right)^4\right\rangle &= 24\sum_{i<j<k<h}\langle s\rangle^4\langle\rho_i\rho_j\rho_k\rho_h\rangle \\ &+36\sum_{i<k<h}\langle s^2\rangle\langle s\rangle^2\langle {\rho_i}^2\rho_k\rho_h\rangle + 6\sum_{i<k}\langle s^2\rangle^2\langle {\rho_i}^2{\rho_k}^2\rangle \\ &+\sum_{i<h}\langle s^3\rangle\langle s\rangle\langle {\rho_i}^3\rho_h\rangle + N\langle s^4\rangle\langle\rho^4\rangle\end{aligned} \tag{S2}$$

Moments of the segment length can be found by direct integration,

$$\langle s^n\rangle = \frac{\int_0^\infty s^{n+2}\exp\left[-\frac{\varepsilon_\parallel}{2\Delta}(s-\Delta\gamma)^2\right]\mathrm{d}s}{\int_0^\infty s^2\exp\left[-\frac{\varepsilon_\parallel}{2\Delta}(s-\Delta\gamma)^2\right]\mathrm{d}s}, \tag{S3}$$

yielding the following expressions:

$$X = \sqrt{2\pi}\exp\left[\gamma^2\Delta\varepsilon_\parallel/2\right]\left(1 + \mathrm{erf}\left[\gamma\sqrt{\frac{\Delta\varepsilon_\parallel}{2}}\right]\right) \tag{S8}$$

To calculate the fourth order correlations in the segment orientations, we expand the propagator $G(\vec{u}_k|\vec{u}_{k-1})$ for the k^{th} segment orientation $\vec{u}_k$ given the orientation of the previous segment $\vec{u}_{k-1}$ in terms of the spherical harmonics,

$$\begin{aligned}G\left(\vec{u}_k|\vec{u}_{k-1}\right) &= \frac{1}{\mathcal{N}}\exp\left[\frac{\varepsilon_b}{\Delta}\left(\vec{u}_k\cdot\vec{u}_{k-1}\right)\right] \\ &= \sum_{l=0}^{\infty}\sum_{m=-l}^{l}\xi_l\,Y_l^{m*}\left(\vec{u}_{k-1}\right)Y_l^m\left(\vec{u}_k\right),\end{aligned} \tag{S9}$$

where $\xi_l = \frac{i_l(\varepsilon_b/\Delta)}{i_0(\varepsilon_b/\Delta)}$ and i_l is the l^{th} modified spherical harmonic Bessel function of the first kind. Eqn (9) combines the usual plane wave expansion in terms of the relative angle between the orientations together with the spherical harmonic addition theorem.[28] The distribution function of the k^{th} segment orientation given the orientation of the 0^{th} segment can be found as a convolution over all intermediate segments. Using the orthonormality of the spherical harmonics this gives,

$$\begin{aligned}G(\vec{u}_k|\vec{u}_0) = &\int \mathrm{d}\vec{u}_1\ldots\mathrm{d}\vec{u}_{k-1} \\ &\sum_{l1\ldots lk}\xi_{l1}\,Y_{l1}^{m1*}(\vec{u}_0)\,Y_{l1}^{m1}(\vec{u}_1)\xi_{l2}\,Y_{l2}^{m2*}(\vec{u}_1)\,Y_{l2}^{m2}(\vec{u}_2)\ldots \\ &m1\ldots mk \\ &\ldots\xi_{lk}\,Y_{lk}^{mk*}(\vec{u}_{k-1})\,Y_{lk}^{mk}(\vec{u}_k) \\ &= \sum_{l=0}^{\infty}\sum_{m=-l}^{l}\left(\xi_l\right)^k\,Y_l^{m*}(\vec{u}_0)\,Y_l^m(\vec{u}_k)\end{aligned} \tag{S10}$$

We find the correlation between segment orientations, with $i \le j$ as,

$$\langle \rho_i \rho_j \rangle = \int \mathrm{d}\vec{u}_i \mathrm{d}\vec{u}_j \rho_i \rho_j \sum_{l,m} \xi_l^{j-i} Y_l^{m*}(\vec{u}_i) Y_l^m(\vec{u}_j) = \frac{1}{3}\xi_1^{j-i}. \quad \text{(S11)}$$

Using the property $\rho Y_l^m(\rho) = a_{l+1}^m Y_{l+1}^m(\rho) + a_l^m Y_{l-1}^m(\rho)$, with $a_l^m = [(l-k)(l+k)/(4l^2-1)]^{1/2}$, we can also calculate the fourth-order correlation function of segment orientations, for $i \le j \le k \le h$,

$$\begin{aligned}\langle \rho_i \rho_j \rho_k \rho_h \rangle &= \int \mathrm{d}\vec{u}_i \mathrm{d}\vec{u}_j \mathrm{d}\vec{u}_k \mathrm{d}\vec{u}_h \rho_i \rho_j \rho_k \rho_h \\ &\sum \xi_{l1}^{j-i} Y_{l1}^{m1*}(\vec{u}_i) Y_{l1}^{m1}(\vec{u}_j) \xi_{l2}^{k-j} Y_{l2}^{m2*}(\vec{u}_j) Y_{l2}^{m2}(\vec{u}_k) \\ &\times \xi_{l3}^{h-k} Y_{l3}^{m3*}(\vec{u}_k) Y_{l3}^{m3}(\vec{u}_h) \\ &= \frac{1}{9}\xi_1^{j-i+h-k}\left(\frac{4}{5}\xi_2^{k-j} + 1\right)\end{aligned} \quad \text{(S12)}$$

Plugging into eqn (S1) and carrying out the summations over indices i, j, k, h yields the two lowest order moments for a chain with N segments in the form,

$$\begin{aligned}\langle {R_Z}^2 \rangle &= C_2^{(1)} \Delta N + C_2^{(0)} + \ldots \\ \langle {R_Z}^4 \rangle &= C_4^{(2)} \Delta^2 N^2 + C_4^{(1)} \Delta N + C_4^{(0)} + \ldots\end{aligned} \quad \text{(S13)}$$

where (…) contains terms that decay exponentially with N. To discretize a continuous wormlike chain with persistence length ℓ_p as an effective discrete stretchable WLC, we numerically solve the following equations to find the effective parameters ε_b, γ, $\varepsilon_\parallel$:

$$C_2^{(1)} = \frac{2}{3}\frac{\langle s \rangle^2 \xi_1}{(1-\xi_1)} + \frac{1}{3}\langle s^2 \rangle = \frac{2}{3}\ell_p \quad \text{(S14)}$$

$$C_2^{(0)} = -\frac{2}{3}\frac{\langle s \rangle^2 \xi_1}{(1-\xi_1)^2} = -\frac{2}{3}{\ell_p}^2 \quad \text{(S15)}$$

$$\begin{aligned}C_4^{(1)} = &\frac{4\langle s \rangle^4 {\xi_1}^2(-25 + 5\xi_1 + 33\xi_2 - 13\xi_1\xi_2)}{15(1-\xi_1)^3(1-\xi_2)} \\ &+ \frac{4\langle s^2 \rangle \langle s \rangle^2 \xi_1 (15 - 23\xi_2 - 14\xi_1 + 22\xi_1\xi_2)}{15(\xi_1 - 1)^2(\xi_2 - 1)} \\ &+ \frac{\langle s^2 \rangle^2 (5 - 13\xi_2)}{15(\xi_2 - 1)} + \frac{8\langle s^3 \rangle \langle s \rangle}{5(1-\xi_1)} + \frac{\langle s^4 \rangle}{5} = -\frac{208}{45}{\ell_p}^3\end{aligned} \quad \text{(S16)}$$

B Projected propagator coefficients for the DSSWLC

In this section we calculate the matrix of coefficients obtained by projecting the Fourier-transformed propagator $\hat{G}_1(\vec{u}, k|\vec{u}_0)$ of the dssWLC model onto the spherical harmonics (eqn (9)), focusing specifically on the case with $j = 0$. We begin by defining the relative orientation vector $\hat{u}$, such that if $\boldsymbol{R}$ is a three-dimensional rotation that places $\vec{u}_0$ on the $\hat{z}$ axis, then $\hat{u} = \boldsymbol{R}\cdot\vec{u}$. Additionally, we define $\hat{u}_0 = \boldsymbol{R}\cdot\hat{z}$. This yields the following identities in terms of the spherical harmonic functions,

$$\begin{aligned}\vec{u}_0 \cdot \hat{z} &= \sqrt{\frac{4\pi}{3}} Y_1^0(u_0) = \sqrt{\frac{4\pi}{3}} Y_1^0(\hat{u}_0) \\ \vec{u}\cdot\vec{u}_0 &= \sqrt{\frac{4\pi}{3}} Y_1^0(\hat{u}) \\ \vec{u}\cdot\hat{z} &= \sqrt{\frac{4\pi}{3}} Y_1^0(u) = \frac{4\pi}{3}\sum_{j=-1}^{1} Y_1^{j*}(\hat{u}_0) Y_1^j(\hat{u})\end{aligned} \quad \text{(S17)}$$

where the last equation is an instance of the spherical harmonic addition theorem.[28]

The propagator can then be expressed as,

$$\begin{aligned}\hat{G}_1 &= F(\hat{u}) \exp\left[H(k, \hat{u}_0, \hat{u})\right] \\ F(\hat{u}) &= \frac{1}{\mathcal{N}} \exp\left\{\frac{\varepsilon_b}{\Delta}(\hat{u}\cdot\hat{z}) + \frac{\eta^2 {\varepsilon_b}^2}{2\Delta\hat{\varepsilon}_\perp}\left[1 - (\hat{u}\cdot\hat{z})^2\right]\right\} \\ H(k, \hat{u}_0, \hat{u}) &= ik\left\{\Delta\gamma\sqrt{\frac{4\pi}{3}} Y_1^0(\hat{u}_0)\right. \\ &\left. + \frac{4\pi\eta\varepsilon_b}{3\hat{\varepsilon}_\perp}\left[Y_1^1(\hat{u}) Y_1^{1*}(\hat{u}_0) + Y_1^{-1}(\hat{u}) Y_1^{-1*}(\hat{u}_0)\right]\right\} \\ &- k^2\left\{\frac{\Delta}{6}\left(\frac{1}{\varepsilon_\parallel} - \frac{1}{\hat{\varepsilon}_\perp}\right)\left[\sqrt{\frac{16\pi}{5}} Y_2^0(\hat{u}_0) + 1\right] + \frac{\Delta}{2\hat{\varepsilon}_\perp}\right\}\end{aligned} \quad \text{(S18)}$$

In order to find the matrix of coefficients for projecting $\hat{G}_1$ onto the spherical harmonics, we assume that this matrix will be truncated at the l_{max} level and proceed to expand the quantity $\exp[H(k, \vec{u}_0, \hat{u})]$ out to the l_{max} order in the wave-vector k. We note that the expansion of a product of two spherical harmonics is given by,[35]

$$\begin{aligned}Y_{l_1}^{j_1} Y_{l_2}^{j_2} = &\frac{(-1)^{j_1+j_2}}{\sqrt{4\pi}} \sum_{l_3=|l_1-l_2|}^{l_1+l_2} \sqrt{(2l_1+1)(2l_2+1)(2l_3+1)} \\ &\times \begin{pmatrix} l_1 & l_2 & l_3 \\ 0 & 0 & 0 \end{pmatrix} \begin{pmatrix} l_1 & l_2 & l_3 \\ j_1 & j_2 & -j_1-j_2 \end{pmatrix} Y_{l_3}^{j_1+j_2}\end{aligned} \quad \text{(S19)}$$

where the parentheses enclose Wigner 3j symbols.[35] The matrix element g_{l,l_0} contains terms that are of order at least $\max(l,l_0)$ in k. Thus, truncating the matrix of coefficients is equivalent to setting a length scale cutoff below which the partition function becomes inaccurate.

The quantity H is a linear combination of terms of the form $Y_a^j(\vec{u}_0) Y^j{}_b(\hat{u})$. Expanding out the exponent yields

$$\exp\left[H(k, \hat{u}_0, \hat{u})\right] = \sum_{a,b,j} h_{a,b}^j Y_a^j(\hat{u}_0) Y_b^j(\hat{u}) \quad \text{(S20)}$$

where $a \ge 0$, $b \ge 0$, $|j| \le \min(a,b)$ and the coefficients $h_{a,b}^j$ are obtained by applying eqn (S19) repeatedly.

We then perform another spherical harmonic expansion to give

$$F(\hat{u}) = \sum_\lambda \xi_\lambda Y_\lambda^0(\hat{u}). \quad \text{(S21)}$$

The coefficients $\xi\lambda = \int F(\hat{u}) Y_\lambda^0(\hat{u}) \mathrm{d}\hat{u}$ are found recursively using the usual formula for the Legendre polynomials:[28]

$$\frac{\lambda+1}{\sqrt{2\lambda+3}} Y_{\lambda+1}^0 = \sqrt{2\lambda+1}\,\hat{\rho}\, Y_\lambda^0 - \frac{\lambda}{\sqrt{2\lambda-1}} Y_{\lambda-1}^0, \quad \text{(S22)}$$

together with the additional recursion,

$$\begin{aligned}I_n &= \int_{-1}^{1} \hat{\rho}^n \exp\left[\alpha\hat{\rho} - \beta\hat{\rho}^2\right] \mathrm{d}\hat{\rho} \\ \frac{-2\beta}{n+1} I_{n+2} &= \frac{1}{n+1}\left[\mathrm{e}^{\alpha-\beta} - (-1)^{n+1}\mathrm{e}^{-\alpha-\beta}\right] \\ &- \frac{a}{n+1} I_{n+1} - I_n,\end{aligned} \quad \text{(S23)}$$

where in this case $\hat{\rho} = \hat{u}\cdot\hat{z}$. All the coefficients are normalized such that $\xi_0 = 1$

The coefficients in the spherical harmonic projection of the propagator (eqn (9)) are given by,

$$g_{l,l_0} = \int Y^0_{l_0}(\vec{u}_0)\,\hat{G}_1(\vec{u},k|\vec{u}_0|)\,Y^0_l(\vec{u})\,\mathrm{d}\vec{u}\mathrm{d}\vec{u}_0 \tag{S24}$$

For convenience we define the tensor,

$$\begin{aligned} M^{a,b,j}_{l,l_0} &= \int \mathrm{d}\vec{u}\mathrm{d}\vec{u}_0\, Y^0_{l_0}(\vec{u}_0)\, Y^{j^*}_a(\hat{u}_0)\, Y^j_b(\hat{u})\, Y^0_l(\vec{u}) F(\hat{u}) \\ g_{l,l_0} &= \sum_{a,b,j} h^j_{a,b} M^{a,b,j}_{l,l_0} \end{aligned} \tag{S25}$$

As our expansion of the propagator is expressed in terms of the relative orientation vector $\hat{u}$ rather than $\vec{u}$, we make use of the spherical harmonics addition theorem to interconvert between them:[28]

$$Y^0_l(\vec{u}) = \sqrt{\frac{4\pi}{2l+1}}\sum_m Y^m_l(\hat{u}_0)\,Y^{m^*}_l(\hat{u}) \tag{S26}$$

Consequently, we have

$$\begin{aligned} M^{a,b,j}_{l,l_0} =& \sqrt{\frac{4\pi}{2l+1}}\sum_m \left\{ \left[\int \mathrm{d}\hat{u}_0\, Y^0_{l_0}(\hat{u}_0)\, Y^m_l(\hat{u}_0)\, Y^{j^*}_a(\hat{u}_0)\right] \right. \\ & \left. \times \left[\sum_\lambda \xi_\lambda \int \mathrm{d}\hat{u}\, Y^j_b(\hat{u})\, Y^0_\lambda(\hat{u})\, Y^{m^*}_l(\hat{u})\right]\right\} \\ =& \sqrt{\frac{(2a+1)(2b+1)(2l_0+1)(2l+1)}{4\pi}} \sum_{\lambda=|l-b|}^{l+b} \xi_\lambda \sqrt{2\lambda+1} \\ & \times \begin{pmatrix} l & l_0 & a \\ 0 & 0 & 0 \end{pmatrix} \begin{pmatrix} l & l_0 & a \\ 0 & j & -j \end{pmatrix} \begin{pmatrix} b & \lambda & l \\ 0 & 0 & 0 \end{pmatrix} \begin{pmatrix} b & \lambda & l \\ j & 0 & -j \end{pmatrix} \end{aligned} \tag{S27}$$

where the coefficients $\xi\lambda$ are found using eqn (S21)–(S23).

C Moments of the end-to-end displacement

Moments of the end-to-end distribution for a chain of length N segments are found *via*,

$$\left\langle R_z^{2n}\right\rangle = (i)^n \frac{\partial^n g^N_{00}}{\partial k^n}. \tag{S28}$$

In a previous work,[25] we showed that such moments can be expressed as an expansion in terms of the chain length,

$$\begin{aligned} \left\langle R_z^2\right\rangle &= C_2^{(1)}\Delta N + C_2^{(0)} + \ldots \\ \left\langle R_z^4\right\rangle &= C_4^{(2)}(\Delta N)^2 + C_4^{(1)}\Delta N + C_4^{(0)} + \ldots \\ \left\langle R_z^{(2n)}\right\rangle &= C_{2n}^{(n)}(\Delta N)^n + C_{2n}^{(n-1)}(\Delta N)^{n-1} + \ldots C_{2n}^{(0)} + \ldots, \end{aligned} \tag{S29}$$

where all terms that decrease exponentially with chain length are dropped. Furthermore, if the three coefficients $C_2^{(1)}$, $C_2^{(0)}$, $C_4^{(1)}$are matched for two chain models, then all moments of the end-to-end distance will match out to an error that scales as $\mathcal{O}(1/N^2)$ as a fraction of the long-length limit. In the appendix of this previous work[25] we employed stone-fence diagrams to calculate the lowest-order moments for the case of a kinked WLC, another form of discrete polymer. The current case of the discrete shearable WLC model yields analogous results, where each block matrix $\boldsymbol{B}_{l_0,l}$ in the propagator for the kinked chain is replaced with a single element g_{l,l_0} for the dssWLC propagator. For completeness, we give the final expressions here, in terms of the derivatives of g_{l,l_0} at $k = 0$:

$$\begin{aligned} \Delta C_2^{(1)} &= \frac{2}{\left(\hat{\xi}_1 - 1\right)} g'_{01}g'_{10} - g''_{00} \\ C_2^{(0)} &= \frac{2}{\left(\hat{\xi}_1 - 1\right)^2} g'_{01}g'_{10} \\ \Delta C_4^{(1)} &= -\frac{12\left(\hat{\xi}_1 - 5\right)}{\left(\hat{\xi}_1 - 1\right)^3} g'^2_{01}g'^2_{10} + \frac{12\left(\hat{\xi}_1 - 3\right)}{\left(\hat{\xi}_1 - 1\right)^2} g''_{00}g'_{01}g'_{10} \\ & -3g''^2_{00} - \frac{24}{\left(\hat{\xi}_1 - 1\right)^2\left(\hat{\xi}_2 - 1\right)} g'_{01}g'_{12}g'_{21}g'_{10} \\ & + \frac{12}{\left(\hat{\xi}_1 - 1\right)^2} g'_{01}g''_{11}g'_{10} - \frac{6}{\hat{\xi}_2 - 1} g''_{02}g''_{20} \\ & + \frac{12}{\left(\hat{\xi}_1 - 1\right)\left(\hat{\xi}_2 - 1\right)} \left[g''_{02}g'_{21}g'_{10} + g'_{01}g'_{12}g''_{20}\right] \\ & + \frac{4}{1 - \hat{\xi}_1}\left[g'''_{01}g'_{10} + g'_{01}g'''_{10}\right] + g''''_{00}, \end{aligned} \tag{S30}$$

where we define $\hat{\xi}_\lambda = \xi_\lambda/\sqrt{2\lambda+1}$.

D Finding effective DSSWLC parameters

For purposes of discretizing a continuous WLC, the parameters ε_b, γ, $\varepsilon_\parallel$, $\varepsilon_\perp$, α for the effective dssWLC model with discretization length Δ are extracted by matching the coefficients $C_2^{(1)} = 2/3$, $C_2^{(0)} = -2/3$, $C_4^{(1)} = -208/45$ to those of the continuous chain.

We note that the coefficients $\hat{\xi}_\lambda$ depend only on ε_b and α. The effective persistence length of the discrete chain is given by,

$$g_{11}(k=0) = \hat{\xi}_1 = \exp(-\Delta/\ell_p^{\mathrm{eff}}) \tag{S31}$$

All the derivatives of matrix elements that enter into eqn (S30) are polynomial functions of γ, ${\varepsilon_\parallel}^{-1}$, ${\hat{\varepsilon}_\perp}^{-1}$, as well as depending on the ξ_λ. We find the effective parameters for the dssWLC according to the following scheme,

1 Fix a value of α.

2 Fix a value of ℓ_p^{eff}.

3 Solve for the appropriate value of ε_b.

4 Calculate coefficients ξ_λ for $1 \le \lambda \le 4$.

5 Match the coefficient $C_2^{(0)}$ to express $\gamma{\hat{\varepsilon}_\perp}^{-1}$ as a quadratic polynomial in γ.

6 Match the coefficient $C_2^{(1)}$ to express $\gamma^2{\varepsilon_\parallel}^{-1}$ as a fourth-order polynomial in γ.

7 Match the coefficient $C_4^{(1)}$, solving an eighth-order polynomial to find an appropriate value of γ.

8 Repeat steps 2–7 to find the lowest value of ℓ_p^{eff} such that a positive real solution exists for all parameters.

The fixed parameter α can then be adjusted to minimize the length-scale of accuracy based on the comparison between the discrete chain structure factor and that of the continuous WLC.

E Non-shearable limit of the DSSWLC

In the limit where the shear modulus goes to infinity, the dssWLC model described in this manuscript reduces to a modified version of the discrete stretchable WLC (defined by eqn (4)). The shear component of the single segment propagator G_1 behaves in this limit as,

$$\exp\Big[-\frac{\varepsilon_\perp}{2\Delta}\big(\vec{R}_i-\big(\vec{R}_i\cdot\vec{u}_{i-1}\big)\vec{u}_{i-1}\big)^2\Big]\xrightarrow{\varepsilon_\perp\to\infty}\frac{1}{|R|^2}\big[\delta\big(\vec{R}_i\cdot\vec{u}_{i-1}-|\vec{R}_i|\big)+\delta\big(\vec{R}_i\cdot\vec{u}_{i-1}+|\vec{R}_i|\big)\big], \tag{S32}$$

where δ is the Dirac delta function. The overall density for a sequence of segments $\vec{R}_1,\ldots,\vec{R}_N$, integrated over the auxiliary orientation vectors $\vec{u}_i$ is then given by,

$$\begin{aligned}P\big(\vec{R}_1\ldots\vec{R}_N\big)\;&=\frac{1}{\mathcal{N}}\sum_{m_1=0}^{1}\ldots\sum_{m_N=0}^{1}\exp\Big\{-\frac{\varepsilon_\parallel}{2\Delta}[R_1-(-1)^{m_1}\gamma\Delta]^2\ldots\\&-\frac{\varepsilon_\parallel}{2\Delta}[R_N-(-1)^{m_N}\gamma\Delta]^2+(-1)^{m_1+m_2}\frac{\varepsilon_b}{\Delta}(\vec{n}_1\cdot\vec{n}_2)\ldots\\&+(-1)^{m_{N-1}+m_N}\frac{\varepsilon_b}{\Delta}(\vec{n}_{N-1}\cdot\vec{n}_N)\Big\}.\end{aligned} \tag{S33}$$

Here we define the normalized bead-to-bead vectors $\vec{n}_i=\vec{R}_i/|\vec{R}_i|$. This summation can be expressed in terms of transfer matrices,

$$\begin{aligned}&P\big(\vec{R}_1\ldots\vec{R}_N\big)=\exp\Big\{-\frac{\varepsilon_\parallel}{2\Delta}\sum_{i=1}^{N}\big(|\vec{R}_i|-\gamma\Delta\big)^2+\frac{\varepsilon_b}{\Delta}\sum_{i=2}^{N}\vec{n}_i\cdot\vec{n}_{i-1}\Big\}\\&\times\vec{A}_1^T B_{1,2}A_2B_{2,3}\ldots A_{n-1}B_{n-1,n}\vec{A}_n\Big/\prod_{i=1}^{N}|\vec{R}_i|^2\\&A_i=\begin{pmatrix}1&0\\0&\exp\big[-2|\vec{R}_i|\gamma\varepsilon_\parallel\big]\end{pmatrix},\quad\vec{A}_i=\begin{pmatrix}1\\\exp\big[-2|\vec{R}_i|\gamma\varepsilon_\parallel\big]\end{pmatrix}\\&B_{i,j}=\begin{pmatrix}1&\exp\Big[-\frac{2\varepsilon_b}{\Delta}\vec{n}_i\cdot\vec{n}_j\Big]\\\exp\Big[-\frac{2\varepsilon_b}{\Delta}\vec{n}_i\cdot\vec{n}_j\Big]&1\end{pmatrix}\end{aligned} \tag{S34}$$

The limiting behavior of this chain can then be described by the free energy function,

$$\begin{aligned}&E\Big(\big\{\vec{R}_i\big\}\Big)=\\&\sum_{i=1}^{N}\Big[-\frac{\varepsilon_b}{\Delta}\vec{n}_i\cdot\vec{n}_{i-1}+\frac{\varepsilon_\parallel}{2\Delta}\big(|\vec{R}_i|-\Delta\gamma\big)^2+\log\big(|\vec{R}_i|^2\big)\Big]\\&-\log\Big(\vec{A}_1^T B_{1,2}A_2B_{2,3}\ldots A_{n-1}B_{n-1,n}\vec{A}_n\Big).\end{aligned} \tag{S35}$$

There are thus two additional terms in the energy compared to the usual formulation of the discrete stretchable WLC (eqn (4)). These terms arise because the energy associated with altering the orientation of the segments in the dssWLC model is controlled by the unit vectors $\vec{u}_i$ rather than the inter-segment vectors directly. The final term results because the infinite shear limit does not prevent a segment from being oppositely oriented to its orientation vector ($\vec{R}_i\cdot\vec{u}_{i-1}=-|\vec{R}_i|$). We note that this last term becomes exponentially small in the limit of stiff, relatively inextensible segments (large $\varepsilon_\parallel$). For very stiff springs ($\varepsilon_\parallel\to\infty$) the additional energy terms vanish (or become constant) and the model reduces to the bead–rod model defined by eqn (1).

The energy function given by eqn (S35) can be implemented in a straight-forward manner for simulating the thermodynamic behavior of the dssWLC model in the $\varepsilon_\perp\to\infty$ limit using Monte Carlo simulations. This formulation eliminates the need to keep track of the auxiliary orientation vectors $\vec{u}_i$, halving the degrees of freedom, and thus resulting in considerable computational savings.

Acknowledgements

We are grateful for helpful discussions with Ekaterina Pilyugina and Jay Schieber. Funding for this project was provided by the Fannie and John Hertz Foundation and the NSF CAREER award.

References

1 O. Kratky and G. Porod, *Recl. Trav. Chim. Pays-Bas*, 1949, **68**, 1106.
2 H. Yamakawa, *Pure Appl. Chem.*, 1976, **46**, 135.
3 J. Marko and E. Siggia, *Macromolecules*, 1995, **28**, 8759.
4 M. Wang, H. Yin, R. Landick, J. Gelles and S. Block, *Biophys. J.*, 1997, **72**, 1335.
5 C. Bouchiat, M. Wang, J. Allemand, T. Strick, S. Block and V. Croquette, *Biophys. J.*, 1999, **76**, 409.
6 J. Abels, F. Moreno-Herrero, T. Van der Heijden, C. Dekker and N. Dekker, *Biophys. J.*, 2005, **88**, 2737.
7 X. Liu and G. Pollack, *Biophys. J.*, 2002, **83**, 2705.
8 L. Lapidus, P. Steinbach, W. Eaton, A. Szabo and J. Hofrichter, *J. Phys. Chem. B*, 2002, **106**, 11628.
9 M. Sano, A. Kamino, J. Okamura and S. Shinkai, *Science*, 2001, **293**, 1299.
10 H. Yamakawa, *Helical wormlike chains in polymer solutions*, Springer, Berlin, 1997.
11 S. Mehraeen, B. Sudhanshu, E. Koslover and A. Spakowitz, *Phys. Rev. E: Stat., Nonlinear, Soft Matter Phys.*, 2008, **77**, 061803.
12 J. Shimada and H. Yamakawa, *Macromolecules*, 1984, **17**, 689.
13 A. Spakowitz and Z. Wang, *Phys. Rev. E: Stat., Nonlinear, Soft Matter Phys.*, 2005, **72**, 041802.
14 A. J. Spakowitz, *Europhys. Lett.*, 2006, **73**, 684.
15 J. Langowski, *Eur. Phys. J. E: Soft Matter Biol. Phys.*, 2006, **19**, 241.
16 J. Sun, Q. Zhang and T. Schlick, *Proc. Natl. Acad. Sci. U. S. A.*, 2005, **102**, 8180.
17 A. Spakowitz and Z. Wang, *Biophys. J.*, 2005, **88**, 3912.
18 D. Head, A. Levine and F. MacKintosh, *Phys. Rev. E: Stat., Nonlinear, Soft Matter Phys.*, 2003, **68**, 061907.
19 T. Kim, W. Hwang, H. Lee and R. Kamm, *PLoS Comput. Biol.*, 2009, **5**, e1000439.
20 M. Somasi, B. Khomami, N. Woo, J. Hur and E. Shaqfeh, *J. Non-Newtonian Fluid Mech.*, 2002, **108**, 227.

21 P. Underhill and P. Doyle, *J. Non-Newtonian Fluid Mech.*, 2004, **122**, 3.
22 M. Rubinstein and R. Colby, *Polymer Physics*, Oxford Univ. Press, New York, NY, 2003.
23 P. Underhill and P. Doyle, *J. Rheol.*, 2005, **49**, 963.
24 P. Underhill and P. Doyle, *J. Rheol.*, 2006, **50**, 513.
25 E. F. Koslover and A. J. Spakowitz, *Macromolecules*, 2013, **46**, 2003, http://pubs.acs.org/doi/pdf/10.1021/ma302056v, http://pubs.acs.org/doi/abs/10.1021/ma302056v.
26 M. Frank-Kamenetskii, A. Lukashin, V. Anshelevich, A. Vologodskii, *et al.*, *J. Biomol. Struct. Dyn.*, 1985, **2**, 1005.
27 Z. Farkas, I. Derényi and T. Vicsek, *J. Phys.: Condens. Matter*, 2003, **15**, S1767.
28 G. Arfken, H. Weber and F. Harris, *Mathematical Methods For Physicists International Student Edition*, Elsevier Science, 2005, ISBN 9780080470696, http://books.google.com/books?id=tNtijk2iBSMC.
29 Y. Zhou and G. Chirikjian, *Macromolecules*, 2006, **39**, 1950.
30 C. Bustamante, J. F. Marko, E. D. Siggia and S. Smith, *Science*, 1994, **265**, 1599, ISSN 00368075, http://www.jstor.org/stable/2884574.
31 C. Cecconi, E. Shank, C. Bustamante and S. Marqusee, *Science*, 2005, **309**, 2057.
32 V. Katritch, C. Bustamante, W. Olson, *et al.*, *J. Mol. Biol.*, 2000, **295**, 29.
33 F. Aumann, F. Lankas, M. Caudron and J. Langowski, *Phys. Rev. E: Stat., Nonlinear, Soft Matter Phys.*, 2006, **73**, 041927.
34 I. Huopaniemi, K. Luo, T. Ala-Nissila and S. Ying, *Phys. Rev. E: Stat., Nonlinear, Soft Matter Phys.*, 2007, **75**, 061912.
35 M. Rose, *Elementary Theory of Angular Momentum*, Dover Books on Physics Series (John Wiley & Sons), 1957, ISBN 9780486684802, http://books.google.com/books?id=Fvf2KgcuzTkC.